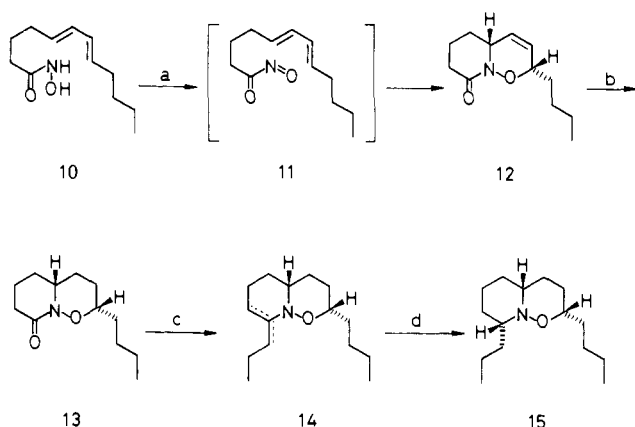
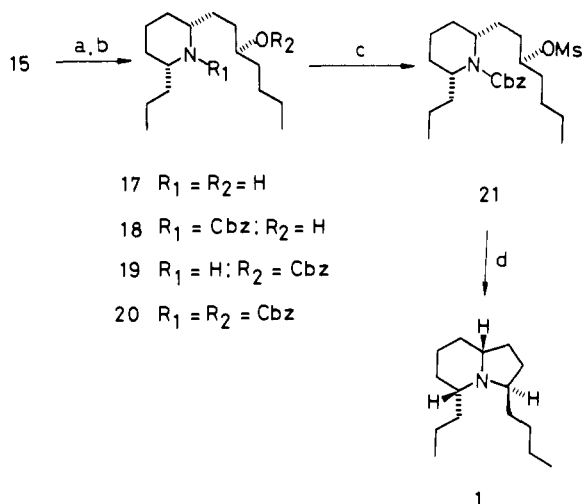


Scheme I

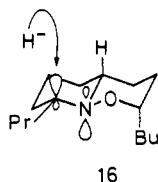


^a (a) *n*-Pr₄N(IO₄), CHCl₃, 0 → 5 °C, 1 h; (b) H₂, 5% Pd/C, MeOH. (c) *n*-PrMgBr, Et₂O, 0 °C → room temperature, 1 h. (d) NaCNBH₃, MeOH, pH 3.8-5.4 (HCl/MeOH, bromocresol green), 0 °C → room temperature, 1 h.

Scheme II^a

^a (a) Zn, AcOH-H₂O (6:4), 60 °C, 90 h; (b) PhCH₂OCOC1, aqueous Na₂CO₃, CHCl₃, 0 °C → room temperature, 2 h; (c) MsCl, NEt₃, CH₂Cl₂, -10 °C, 5 min; (d) H₂ (1 atm), 5% Pd/C, MeOH, room temperature, 5 h.

The exclusive formation of **15** can be rationalized to be a result of stereoelectronically controlled reaction of the transient iminium salt generated from **14** under acidic conditions. Due to inversion at nitrogen, there are thus four possible transition states¹² which maintain maximum orbital overlap with respect to the approaching hydride ion and the developing nitrogen lone pair. Two of these are boat shaped and the other two are of more stable chair shape. One of the latter is disfavored due to a strong peri interaction between the butyl group and the incoming hydride ion. On the other hand, transition state **16** can accommodate the entering



hydride ion without steric interference of the 2-alkyl side chain thereby leading to **15**.

With the required stereochemistry thus established, the only requirement in order to complete the synthesis was constructing

the pyrrolidine moiety of the target molecule. Reductive cleavage (Zn, aqueous AcOH) of the N-O bond in **15** gave the amino alcohol **17** (85%), mp 52-55 °C. Exposure of this material to benzyl chloroformate in an alkaline solution furnished the hydroxy carbamate **18** (36%), along with **19** (24%) and **20** (25%), the latter two product of which could easily be hydrogenated back to the amino alcohol **17**. Thus actual yield of **18** based on recovered **17** was 71%.

Finally, the hydroxy carbamate **18** was converted to the mesylate **21** (MsCl, NEt₃, -10 °C, ca. 5 min; 83%) which upon hydrogenation (Pd/C, MeOH, 1 atm) provided GTX 223AB (**1**) in 81% yield as the sole product. Synthetic material thus prepared was found to have identical spectra (¹H NMR, ¹³C NMR,¹³ and mass¹⁴) with those of natural GTX 223AB.^{15,16}

Acknowledgment. We thank Dr. H. Shindo, Tokyo College of Pharmacy, for his helpful discussion in estimation of ΔG[‡].

(13) The ¹³C NMR spectrum (CDCl₃, 67.8 MHz) of synthetic GTX 223AB was as follows: δ 14.2 (q), 14.5 (q), 19.0 (t), 23.0 (t), 24.6 (t), 25.1 (t), 26.4 (t), 29.1 (t), 30.0 (t), 30.8 (t), 32.2 (t), 35.8 (t), 56.8 (d), 58.6 (d), 59.3 (d).

(14) The mass spectrum of synthetic GTX 223AB was as follows: *m/z* (relative intensity) 223 (2), 222 (3), 181 (14), 180 (99), 167 (14), 166 (100), 124 (6), 122 (3), 81 (6), 55 (13); exact mass calcd for C₁₅H₂₉N, *m/z* 223.2300, found 223.2297.

(15) We thank Drs. J. W. Daly, NIH, and T. Tokuyama, Osaka City University, for the ¹³C NMR data and ¹H NMR spectrum of natural GTX 223AB.

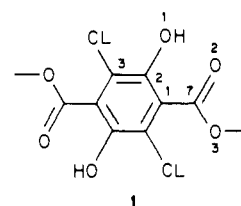
(16) The mass spectrum of natural GTX 223AB has appeared in ref 2.

Internal Molecular Motion as Forerunner of a Phase Change Involving Conformational Isomerization

Qing-Chuan Yang,[†] Mary Frances Richardson,[‡] and Jack D. Dunitz*

Organic Chemistry Laboratory of the
Swiss Federal Institute of Technology
CH-8092 Zürich, Switzerland
Received March 4, 1985

The notion that the vibrational behavior of a molecule in its electronic ground state is related to the pathways for its unimolecular reactions is intuitively appealing.¹ Experimental evidence relevant to this question is, however, hard to come by. Nevertheless, information about internal motions of molecules in crystals can be obtained, in principle and sometimes in practice, by analysis of the anisotropic Gaussian displacement parameters from diffraction studies.² In this paper we describe variable-temperature x-ray diffraction results that show a connection between internal molecular motion and conformational isomerization for dimethyl 3,6-dichloro-2,5-dihydroxyterephthalate (**1**).



The thermally induced solid-state transformation of a yellow into a white crystalline modification of **1** was observed by Hantzsch³ and studied extensively in recent years.⁴⁻⁶ The yellow

[†] On leave from Peking University, China.

[‡] On leave from Brock University, St. Catharines, Ontario, Canada.

(1) See: Swanson, B. I. *J. Am. Chem. Soc.* **1976**, *98*, 3067-3071 for a more formal statement of the relationship between molecular vibrations and reaction coordinates.

(2) Trueblood, K. N.; Dunitz, J. D. *Acta Crystallogr., Sect. B* **1983**, *39B*, 120-133.

(3) Hantzsch, A. *Chem. Ber.* **1915**, *48*, 797-816.

(4) Curtin, D. Y.; Byrn, S. R. *J. Am. Chem. Soc.* **1969**, *91*, 6102-6106.

(12) Stevens, R. F.; Lee, A. W. *J. Am. Chem. Soc.* **1979**, *101*, 7032.

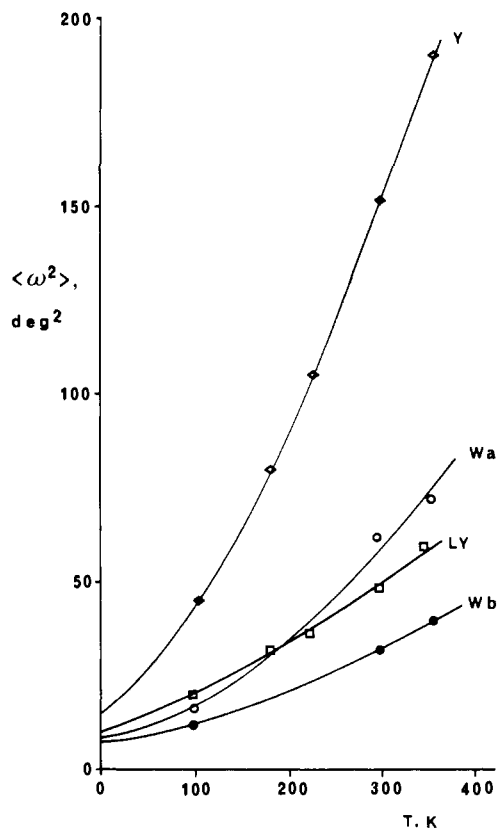


Figure 1. Mean square libration of the carbomethoxy group as a function of temperature. The zero-point motion was calculated from the expression $\langle \omega_0^2 \rangle = h/8\pi^2 I \nu$, where h is Planck's constant, I is the moment of inertia of the librating group, and ν is the librational frequency. To a sufficient degree of accuracy, the estimated standard deviations for each point are: Y, $\sigma = 10.5 + 0.02\langle \omega^2 \rangle$; LY, $\sigma = 2.8 + 0.15\langle \omega^2 \rangle$; Wa, $\sigma = 3.7 + 0.13\langle \omega^2 \rangle$; Wb, $\sigma = 2.5 + 0.22\langle \omega^2 \rangle$.

form contains centrosymmetric, essentially planar molecules **Y1** with intramolecular hydrogen bonds between the hydroxyl groups and the carbonyl oxygen atoms of the vicinal carbomethoxy groups. In contrast, the white form **W1** contains two crystallographically inequivalent centrosymmetric molecules, in both of which the carbomethoxy groups are tilted with their planes nearly perpendicular to the plane through the benzene ring. The hydrogen bonds between the hydroxyl and carbomethoxy groups are intermolecular here.

This system seemed a suitable one for the study of the relationship between thermal motion, isomerization, and phase change.⁷ New diffraction data for **Y1** and **W1** have been measured at several temperatures between 100 and 350 K. Similar measurements have also been made for a new light yellow modification **LY1** which seems to have eluded detection up till now.⁸ Crystals of **LY1** contain centrosymmetric molecules with the carbomethoxy group neither coplanar with the benzene ring, as in **Y1**, nor perpendicular to it, as in **W1**, but in an intermediate orientation, tilted out of the ring plane by approximately 40°. The

(5) Byrn, S. R.; Curtin, D. Y.; Paul, I. C. *J. Am. Chem. Soc.* **1972**, *94*, 890–898.

(6) Swiatkiewicz, J.; Prasad, P. N. *J. Am. Chem. Soc.* **1982**, *104*, 6913–6918.

(7) Our attention was first drawn to this system by Professor K. Venkatesan (I.I.S., Bangalore) during a study visit to Zürich.

(8) Obtained together with **Y1** and **W1** by crystallization from ethanol or ether. Triclinic crystals, $a = 3.8980$ (4) Å, $b = 8.034$ (2) Å, $c = 9.491$ (2) Å, $\alpha = 70.42$ (2)°, $\beta = 89.10$ (1)°, $\gamma = 86.68$ (2)° at 295 K, space group $P\bar{1}$, $Z = 1$. Structure analysis and refinement based on 1208 reflection intensities measured with Mo K α radiation to $\theta = 27^\circ$ at 295 K with parallel measurements at 343, 226, 179, and 97 K. The final R was 0.027 with all atoms except hydrogens refined anisotropically. Similar measurements were made on **Y1** at 353, 296, 230, 180, and 105 K and **W1** at 353, 296, and 98 K. Refinement of these structures yielded R factors of 0.035 or less. Full details of the structure determinations and results will be published elsewhere.

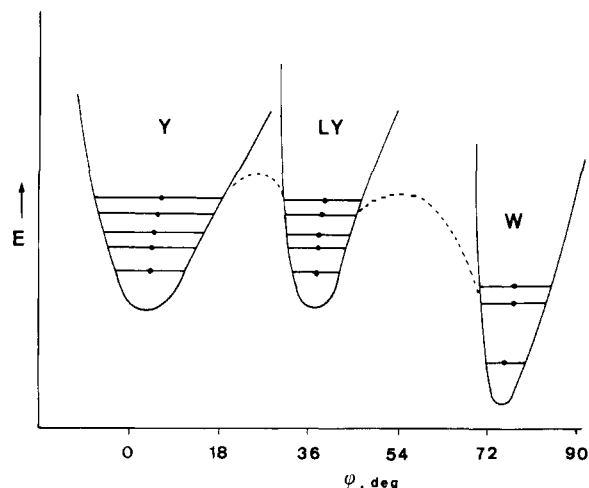


Figure 2. Energy as a function of torsion angle ϕ . The solid curves are based on the experimental data and show the potential energy curves for **Y1**, **LY1**, and **W1**. The horizontal lines represent $\phi \pm \langle \omega^2 \rangle^{1/2}$, and the point in the center of each line shows the value of ϕ at a given temperature. The dashed curves crudely represent the energy changes accompanying carbomethoxy rotation at a defect in the crystal structure.

hydroxyl groups are intramolecularly hydrogen bonded to the carbonyl oxygen atoms, as in **Y1**, and the overall molecular packing is similar to that of **Y1** as well.

LY1 also undergoes phase changes upon heating. Single crystals of **LY1** usually give polycrystalline **W1** on warming to 100 °C, but both **W1** and single crystalline **Y1** regions are occasionally produced from one and the same crystal specimen.

Molecular motion was analyzed in terms of **T** and **L** tensors for the rigid-body motions of the molecule as a whole, plus an internal libration ω of the carbomethoxy group about the C1–C7 axis.⁹ Figure 1 shows $\langle \omega^2 \rangle$ as a function of temperature for each of the molecules. At all temperatures the carbomethoxy group libration is greater in **Y1** than in the other two forms, and it also increases more rapidly with temperature.

The rigid-body librational eigenvalues L1, L2, and L3 increase approximately linearly with temperature in each case. There is thus no evidence for the “softening”¹³ which would be expected if the phase transition involved cooperative motion of a large number of molecules. Rather, since the ability of **Y1** to undergo a phase transition seems to depend on the crystal history,^{5,6} the phase transition is probably defect controlled, as suggested by Swiatkiewicz and Prasad on the basis of phonon and emission spectroscopy.⁶ The $\langle \omega^2 \rangle$ values in Figure 1 suggest that the phase transition may actually be initiated by isomerization. Macroscopic growth of the new phase would then depend on the presence of suitable nucleation sites in the crystal.

In Figure 2 we plot potential energy increment as a function of the torsion angle C2–C1–C7–O2 (ϕ).¹⁴ The three curves (solid lines) with their minima at $\sim 5^\circ$, 40° , and 75° are based on the

(9) Computer program THMV by Schomaker and Trueblood,¹⁰ which includes the Dunitz–White model for internal motions¹¹ plus correlations between these and the rigid-body motions.¹²

(10) Schomaker, V.; Trueblood, K. N. *Acta Crystallogr., Sect. B* **1968**, *24B*, 63–76.

(11) Dunitz, J. D.; White, D. N. *J. Acta Crystallogr., Sect. A* **1973**, *29A*, 93–94.

(12) Schomaker, V.; Trueblood, K. N. *Acta Crystallogr., Sect. A* **1984**, *40A*, suppl. C-339.

(13) A soft mode is a vibrational mode whose frequency goes toward zero as the temperature approaches the phase transition temperature: strictly applicable only to displacive transitions in solids where thermal expansion leads to a softening of the intermolecular potential.

(14) ϕ increases from 3.9 to 6.1° for **Y1** as the temperature increases from 105 to 353 K. Similar increases are observed for the other molecules. Thus the minima at $\phi \sim 5, 40,$ and 75° in the energy curves show anharmonicity in the sense indicated in Figure 2. Compare triclinic ferrocene, where the rotation angle between the two rings increases from about 8.7 to 9.7° (becoming more staggered), between 101 to 148 K.¹⁵

(15) Seiler, P.; Dunitz, J. D. *Acta Crystallogr., Sect. B* **1979**, *35B*, 2020–2032.

φ and $\langle\omega^2\rangle$ values obtained for the three crystal modifications at the various temperatures. The curve for **W1** represents the average over the two independent molecules. The quantity $\langle\omega^2\rangle^{1/2}$ corresponds to the half-width of a parabolic energy well at the height $RT/2$ above its minimum.¹⁶ The relative displacements of the three curves along the energy coordinate depend on the temperature, **Y1** being the most stable at room temperature and **W1** the most stable above about 375 K, as shown in Figure 2. The **Y1** and **LY1** curves are drawn at the same height since the phase transitions from **Y1** to **LY1** and from **LY1** to **Y1** have both been observed at about 375 K. The dashed curves connect the experimental energy wells and may be taken to portray in an approximate way the energy dependence on φ at a defect in the crystal and in a still more approximate way the energy profiles for the phase transformation.¹⁷ At the temperature corresponding to the transformation of **Y1** to **W1** (380–410 K)⁵ the extrapolated value for $\langle\omega^2\rangle^{1/2}$ is quite sufficient to carry it across the barrier to **LY1**, which would then be an intermediate on the way to **W1**. This would agree with an earlier suggestion⁶ that some intermediate structure might be present in the initial stages of the phase transition, before nucleation of **W1** sets in.

Further studies including high-temperature single-crystal NMR work are in progress on this interesting system.

Acknowledgment. We thank Professors I. C. Paul and D. V. Curtin for giving us a sample of **1**, Paul Seiler for assistance with the diffractometer measurements, and the Swiss National Science Foundation for a scientific exchange fellowship for M.F.R.

(16) Shmueli, I.; Kroon, P. A. *Acta Crystallogr., Sect. A* **1974**, *30A*, 768–771.

(17) The reaction paths are certainly more complicated than suggested by Figure 2, but the φ coordinate must represent an important component.

Kinetics of Iron(III) Porphyrin Catalyzed Epoxidations

Teddy G. Traylor,* James C. Marsters, Jr., Taku Nakano, and Beth E. Dunlap

Department of Chemistry D-006
University of California, San Diego
La Jolla, California 92093
Received April 19, 1985

The discovery of model iron(III) porphyrin catalyzed oxidations which mimic the enzymatic epoxidation and hydroxylation reactions catalyzed by cytochrome P-450 has stimulated much interest in the kinetics and mechanisms of these model reactions.^{1–6} These studies require stable catalysts, absence of interfering by-products, and oxidants that are soluble and highly reactive toward the catalyst but not toward the alkene. Although iron(III) tetraphenylporphyrin is rapidly destroyed during catalytic epoxidation by peracids or iodosylbenzenes,⁶ the introduction of bulky and electronegative substituents on the phenyl rings has been shown to greatly reduce this catalyst destruction.^{7,8} Peracids are not sufficiently reactive with iron(III) porphyrins and they react directly with alkenes.^{8–10} Iodosylbenzene is much more reactive

(1) Groves, J. T.; Nemo, T. E.; Myers, R. S. *J. Am. Chem. Soc.* **1976**, *98*, 859–865.

(2) (a) Groves, J. T.; Nemo, T. E. *J. Am. Chem. Soc.* **1983**, *105*, 5786–5791. (b) Groves, J. T.; Haushalter, R. C.; Nakamura, M.; Nemo, T. E.; Evans, B. J. *Ibid.* **19818**, *103*, 2884–2886.

(3) (a) Smegal, J. A.; Hill, C. L. *J. Am. Chem. Soc.* **1983**, *105*, 3515–3521. (b) Schardt, B. C.; Hill, C. L. *Inorg. Chem.* **1983**, *22*, 1563–1565.

(4) (a) Nee, M. W.; Bruice, T. C. *J. Am. Chem. Soc.* **1982**, *104*, 6123–6125. (b) Shannon, P.; Bruice, T. C. *Ibid.* **1981**, *103*, 4580–4582.

(5) Collman, J. P.; Brauman, J. I.; Meunier, B.; Raybuck, S. A.; Kodadek, T. *Proc. Natl. Acad. Sci. U.S.A.* **1984**, *81*, 3245–3248.

(6) Smith, J. R. L.; Sleath, P. R. *J. Chem. Soc., Perkin Trans. 2* **1982**, 1009–1015.

(7) Chang, C. K.; Ebina, F. *J. Chem. Soc., Chem. Commun.* **1981**, 778.

(8) Traylor, P. S.; Dolphin, D.; Traylor, T. G. *J. Chem. Soc., Chem. Commun.* **1984**, 279–280.

(9) (a) Traylor, T. G.; Lee, W. A.; Stynes, D. V. *J. Am. Chem. Soc.* **1984**, *106*, 755–765. (b) Traylor, T. G.; Lee, W. A.; Stynes, D. V. *Tetrahedron* **1984**, *40*, 553–568.

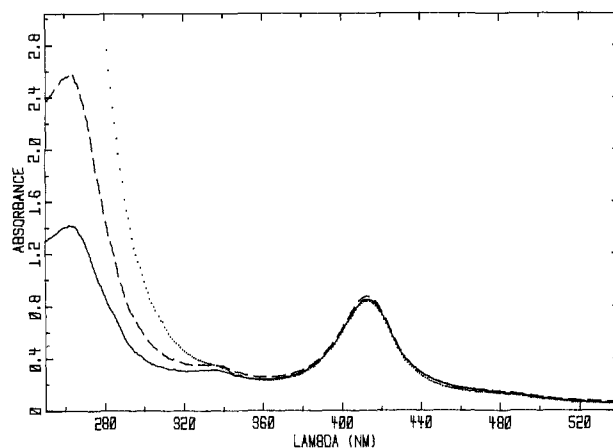


Figure 1. Spectra of reactants and product solutions in $\text{CH}_2\text{Cl}_2/\text{CH}_3\text{OH}/\text{H}_2\text{O}$ (80:18:2). (···) Computer sum of a solution 8.9×10^{-6} M TDCPPFeCl and a solution of 0.5 M norbornene and 10^{-3} M $\text{F}_5\text{C}_6\text{IO}$. (—) Spectrum of a solution originally having these concentrations after a kinetic run. (---) Spectrum of the same solution after addition of a second aliquot of the $\text{F}_5\text{C}_6\text{IO}$ to make the solution again 10^{-3} M in this oxidant. The spectrum was taken after the second kinetic run. Solvent base line was subtracted from all spectra.

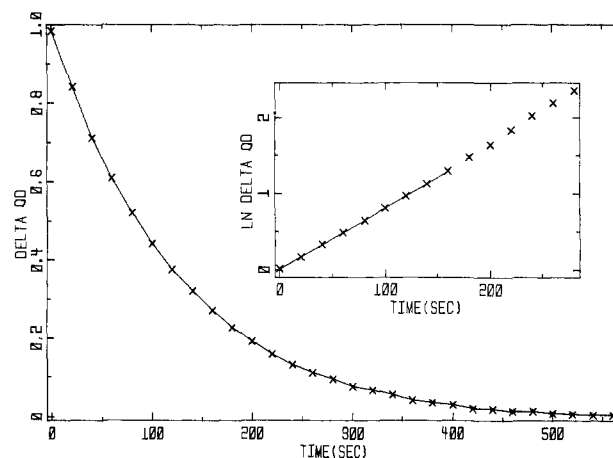


Figure 2. Plots of $A - A_\infty$ and $\ln(A - A_\infty)$ vs. time for a solution of 4.2×10^{-6} M TDCPPFeCl, 1.0 M norbornene, and 10^{-3} M $\text{F}_5\text{C}_6\text{IO}$ in $\text{CH}_2\text{Cl}_2/\text{CH}_3\text{OH}/\text{H}_2\text{O}$ (80:18:2) at 25 °C. Only one of every 20 points is plotted. Rate data are calculated using all points.

toward the catalysts than toward alkenes.⁸ However, iodosylbenzenes are insoluble in methylene chloride, ketones, etc.

We wish to report oxidant systems that meet all the criteria for kinetic studies of very rapid, high turnover catalyzed epoxidation without catalyst destruction, along with preliminary kinetic results with these systems.

Pentafluoriodosylbenzene (PFIB)^{8,11} reacts directly with only the most strained or electron-rich alkenes but reacts very rapidly with iron(III) porphyrins even in methylene chloride where it is insoluble. However, it dissolves readily in alcohols where its reactivity is reduced. Addition of water and methylene chloride increases the reaction rate. Systems we have found convenient for rapid oxidations are methylene chloride/trifluoroethanol/water (80:18:2) or methylene chloride/methanol/water (80:18:2). Concentrations of PFIB up to 0.03 M are obtainable.

In these solvent systems PFIB reacts very slowly, if at all, with alkenes but very rapidly with the catalysts as shown below.¹²

(10) Swern, D. *J. Am. Chem. Soc.* **1947**, *69*, 1692–1698.

(11) (a) Schmeiser, M.; Dahman, K.; Sartori, P. *Chem. Ber.* **1967**, *100*, 1633. (b) Note! Collman, J. P.^{11c} recently reported an explosion of pentafluoriodosylbenzene. This compound should be handled in small quantities and not heated. (c) Collman, J. P. *Chem. Eng. News* **1985**, *63*, 2.

(12) In either this or the methanol solvent system, iron(III) tetraphenylporphyrin and iron(III) tetramesitylporphyrin are destroyed during the kinetic runs.